Electronic Supplementary Material (ESI) for ChemComm.

Supporting Information: Ultra-small Mo-Pt subnanoparticles enable CO_2 hydrogenation at room temperature and atmospheric pressure

Augie Atqa[a], Masataka Yoshida, [a] Masanori Wakizaka, [c] Wang-Jae Chun, [d] Akira Oda, [e] Takane Imaoka, * [a] [b] and Kimihisa Yamamoto* [a] [b]

[a] Institute of Innovative Research
Tokyo Institute of Technology
Yokohama 226-8503 (Japan)

[b] JST ERATO Yamamoto Atom Hybrid Project
Tokyo Institute of Technology
Yokohama 226-8503 (Japan)

[c] Graduate School of Photonic Science
Chitose Institute of Science and Technology
Chitose 066-0012 (Japan)

[d] Graduate School of Arts and Sciences
International Christian University
Tokyo 181-8585 (Japan)

[e] Graduate School of Engineering
Nagoya University
Nagoya 464-8603 (Japan)

Correspondence E-mails: yamamoto@res.titech.ac.jp (K.Y.), timaoka@res.titech.ac.jp (T.I.)

Materials and Methods

Subnanoparticle Synthesis. The TPM-DPAG4 dendrimer template was synthesised according to the previous reports.[1] All of the subnanoparticles were synthesised in three steps: (A) complexation of metal ions, (B) supporting of metal-dendrimer complex, and (C) reduction. (A) The complexation condition of TPM-DPAG4 vs $MoCl_5$ (and $PtBr_4$) was based on the previous reports.[2,3] (B) The $Mo_{12}O_x$, Pt_{12}, and $Mo_4Pt_8O_x$ precursors (0.5 wt.%) were then supported on TiO_2 and dried *in vacuo* for 1 h. (C) The obtained samples were reduced at 500 ºC for 30 min under an H_2 (100 ml/min, 99.99999%) atmosphere on a quartz boat in a furnace at a heating rate of 24 ºC/min. Before and after the reduction, the samples were handled under an Ar atmosphere.

HAADF-STEM Observation and Ultra-small EDS Analysis. High-angle annular dark-field scanning transmission electron microscopy (HAADF-STEM) and ultra-small energy dispersive X-ray spectrometry (EDS) analysis were performed using a JEOL JEM-ARM200F ACCELARM (accelerating voltage: 80 kV) with a spherical aberration-corrected probe. The analytes were dispersed in THF, dropped onto micro Cu grids with carbon filaments (Nisshin EM), and dried for >12h *in vacuo* at room temperature.

XPS Analysis. X-ray photoelectron spectroscopy (XPS) was performed using a ULVAC PHI VersaProbe III. A monochromated Al 1486.6 eV at 49.5 W was used as an X-ray source (beam diameter 200.0 μm). The neutraliser parameter was set to 0.3 V, 3.0 μA. All samples were stored and prepared under an Ar atmosphere and transferred to XPS using a transfer vessel.

XAFS Studies (including *in situ* XAFS). X-ray absorption fine structure (XAFS) experiments were performed at KEK-IMSS-Photon Factory, Tsukuba, Japan. The beamline BL9C (ring energy: 2.5 GeV, 450 mA) was used for Pt L_3-edge measurement, and NW10A (ring energy: 6.5 GeV, 50 mA) was used for Mo K-edge measurement (including *in situ* experiments). X-rays were monochromated by channel-cut monochromators Si(111) at BL9C and Si(311) at NW10A. The ionisation chamber for I_0 was filled with Ar/N_2 15/85 for BL9C and 50/50 for NW10A. The ionisation chamber for I was filled with Ar 100% for BL9C and Kr 100% for NW10A. The fluorescence X-rays were detected using 3-element Si-SDD (BL9C) and 19-element Ge-MSSD (NW10A). MoO_2 and Mo_2C were pelletised by mixing with BN (ϕ 10 mm). The samples ($Mo_{12}O_x/TiO_2$, Pt_{12}/TiO_2, and $Mo_4Pt_8O_x/TiO_2$) were pelletised above the BN pellets. XAFS analyses were performed using REX2000 software (Rigaku Co., ltd., Japan).[4]

***In situ* DRIFTS.** *In situ* diffused reflectance infrared Fourier transform spectroscopy (DRIFTS) measurements were performed using a JASCO FT/IR-6600 spectrometer with a Mercury-Cadmium-Tellurium (MCT) detector (resolution: $2cm^{-1}$, 64 scans, DRIFT mode). Samples were pretreated with H_2 (100%, 20 ml/min) at 150 ºC. After cooling to room temperature, CO_2 (100%, 20 ml/min) was introduced.

Low-temperature CO_2 hydrogenation evaluation. Low-temperature CO_2 hydrogenation (RT-150 ºC) was conducted using a BELCAT-II instrument under atmospheric pressure. Samples (150 mg each) were packed into a continuous flow reactor and pretreated under H_2 gas flow (20 ml/min) at 150°C for 1 hour. After cooling to room temperature, the reactor was purged using Ar gas (20 ml/min) for 1 hour. Then, the gases (CO_2 10 ml/min, H_2 10 ml/min) were introduced. The reaction temperature was elevated by 10 °C per step until 150 °C (each step was held for 30 min). The gases were detected using a GC-FID (minimum detection 0.1 ppm) with Methanizer (Converting CO and CO_2 to CH_4 to be detectable by FID) (Carrier gas: Ar, column: Shincarbon ST 50-80 (6 m×1 mm ID), column temperature: 200 °C, FID temperature: 200 °C, Methanizer temperature: 400 °C). Calibration was performed using CO/Ar gas (10%). The mass spectrum of H_2O (m/z 18) was monitored using a quadrupole mass spectrometer (BELMASS II, Microtrac-Bel Japan Inc., detection limit: <1 ppm).

DFT calculation. In order to analyse the adsorption mechanism of CO of each subnanoparticle on the TiO_2 surface, we performed ab-initio calculation based on density functional theory (DFT) calculation. We obtained the most stable unit cell structure from the Materials Project[5] database to construct a slab model of the TiO_2(101) surface. The program package used was the Vienna ab initio simulation package (VASP 5.4.1).[6-9] The projector-augmented wave (PAW) method [10,11] was used for solving the Kohn-Sham equations, and the generalised gradient approximation of Perdew, Burke, and Ernzerhof (GGA-PBE) [12] was used for calculating exchange and correlation energies. The system must satisfy periodic boundary conditions for calculations using plane wave basis sets. The coordinates of the lower atoms in the slab model are fixed. A vacuum space of 25 Å length is placed on the surface. The k-point spacing was set to $2\pi \times 0.05$ Å^{-1}. The cutoff energy of the plane-wave basis set was 500 eV, and the convergence condition for the self-consistent field (SCF) loop was set to 1×10^{-6} eV. As the convergence condition for structural optimisation, the threshold of the forces on each atom was set to 5×10^{-2} eV/Å. Spin-polarised calculations are performed. We performed all calculations taking collinear spin polarisation into account.

Supplementary Figures

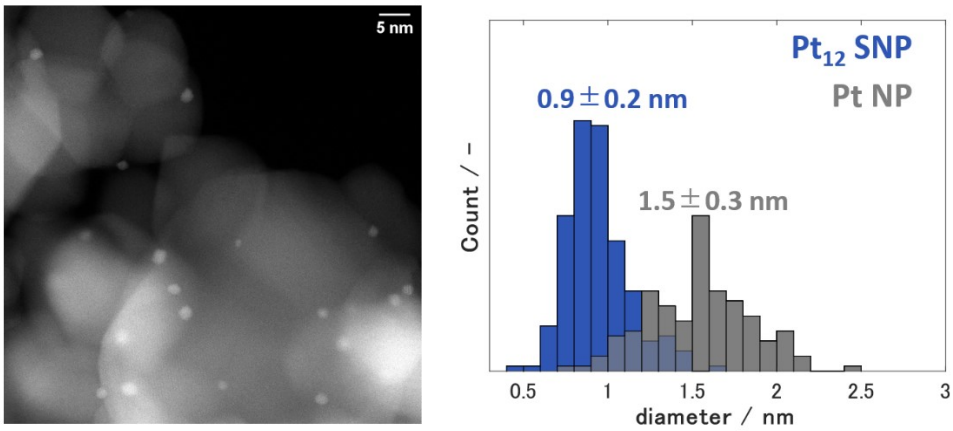

Fig. S1 HAADF-STEM observation of the Pt nanoparticles prepared from Pt_{12} subnanoparticles supported on TiO_2 (**left**) and size distribution comparison of Pt nanoparticles and Pt_{12} subnanoparticles supported on TiO_2 (**right**).

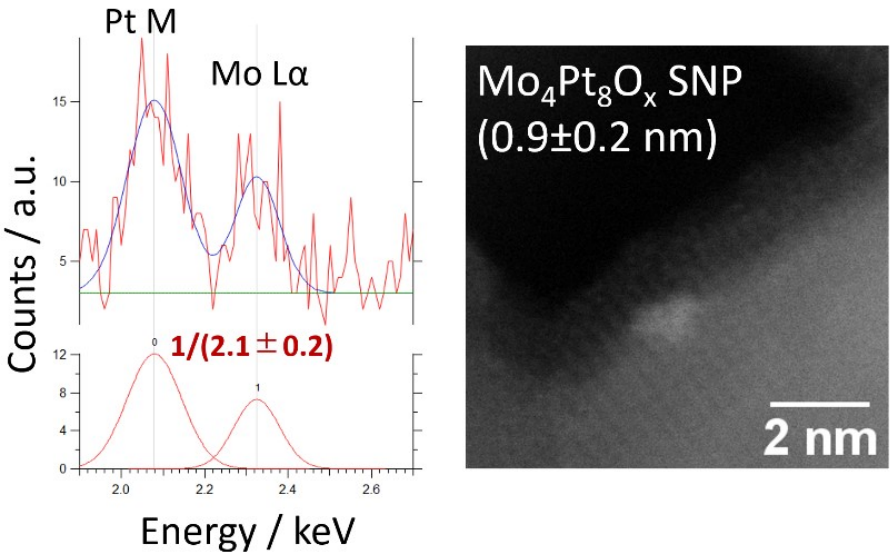

Fig. S2 An example of ultra-small STEM-EDS analyses of one particle region. The average single-particle composition was determined to be Mo: Pt = 1:(2.1±0.2) by the analyses on more than 30 particles.

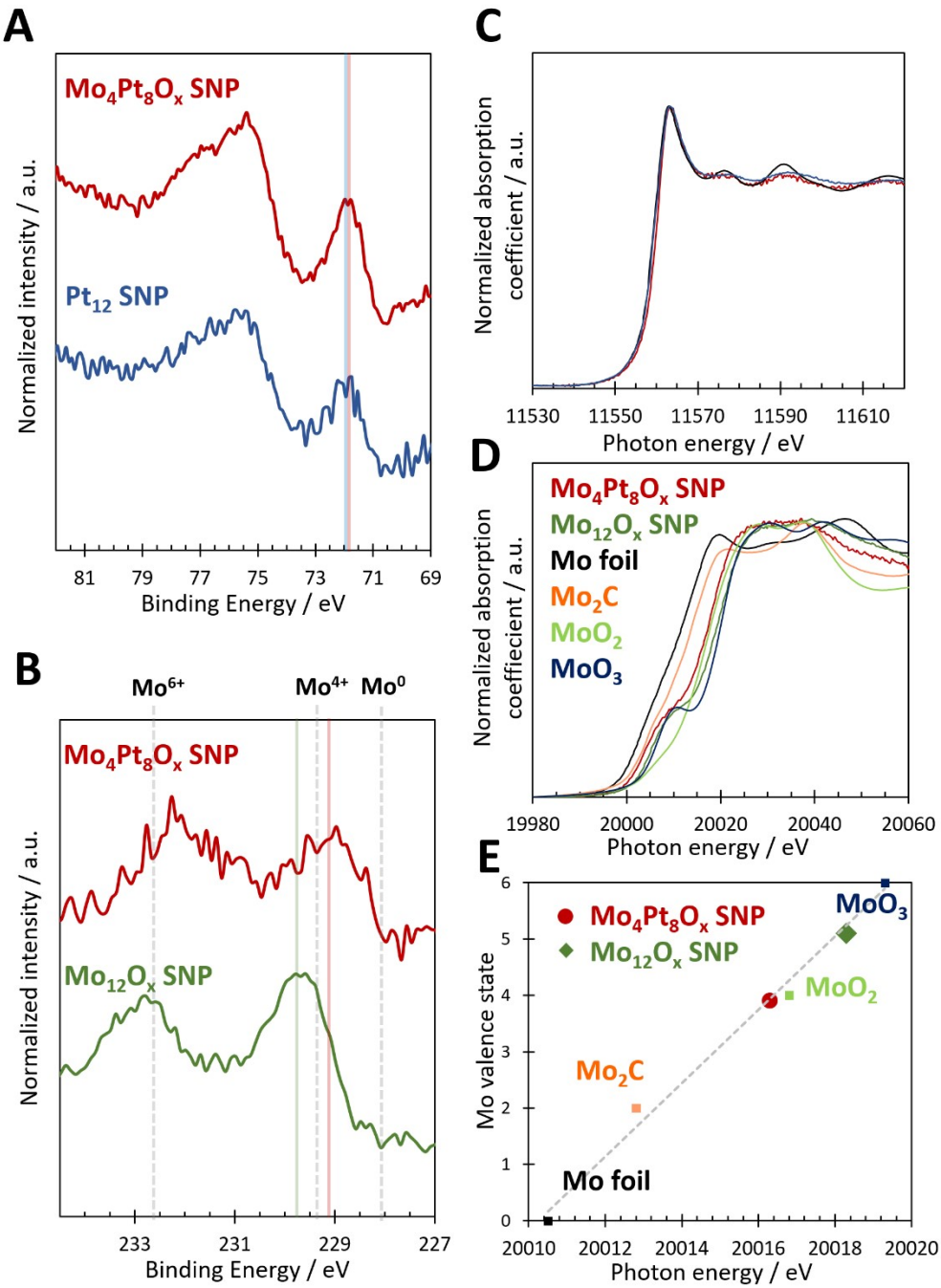

Fig. S3 XPS analysis of Pt4f of $Mo_4Pt_8O_x$, Pt_{12} subnanoparticles (**A**), and Mo3d of $Mo_4Pt_8O_x$, $Mo_{12}O_x$ subnanoparticles (**B**) supported on TiO_2 (All spectra were calibrated using $Ti2p_{3/2}$ 459.5 eV and the estimated error was estimated to be ±0.1 eV). Pt L_3-edge XANES spectra of $Mo_4Pt_8O_x$ & Pt_{12} subnanoparticles (**C**), Mo K-edge XANES spectra of $Mo_4Pt_8O_x$ & $Mo_{12}O_x$ subnanoparticles (**D**) supported on TiO_2. A linear interpolation result of Mo K-edge XANES spectra to obtain the average valence states of Mo species inside the subnanoparticles (**E**).

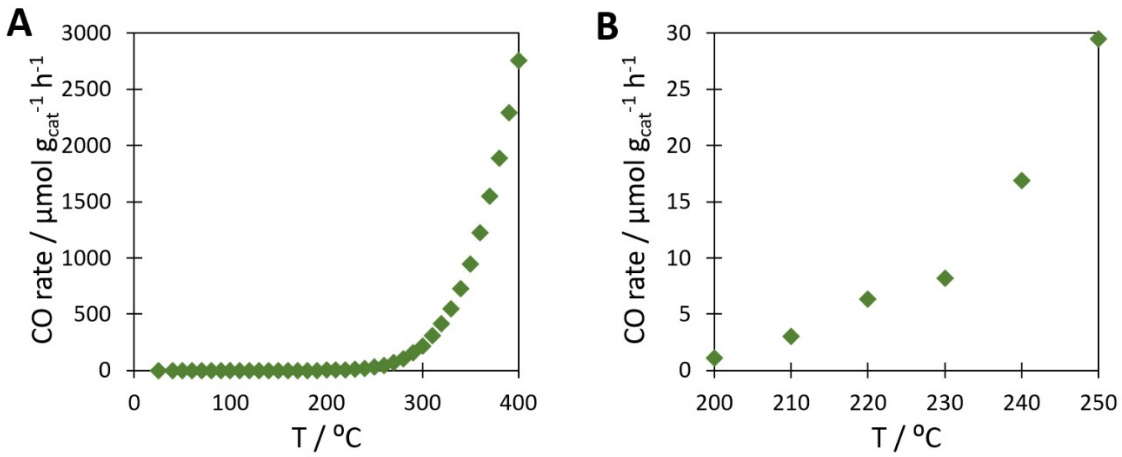

Fig. S4 CO_2 hydrogenation over $Mo_{12}O_x$ subnanoparticles supported on TiO_2 (**A**). CO_2 hydrogenation with a temperature range from 200-250 ºC (**B**). Reaction condition: Catalyst used 150 mg (0.4 wt.%), CO_2 10 ml/min, H_2 10 ml/min, 1 bar (pre-treatment H_2 20 ml/min, 150 ºC, 1h.)

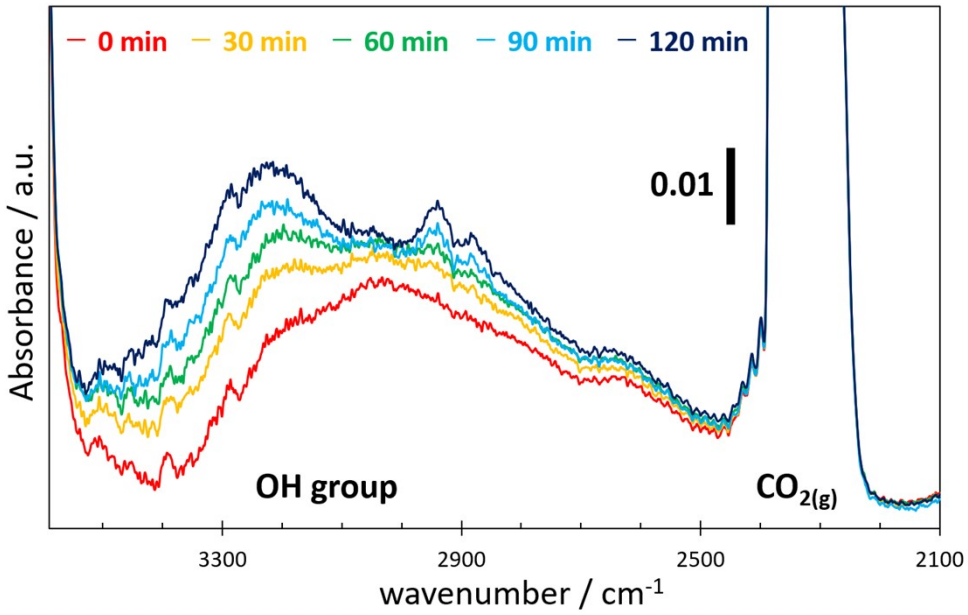

Fig. S5 *Operando* DRIFTS spectra of CO_2 hydrogenation at room temperature and atmospheric pressure employing $Mo_4Pt_8O_x$ subnanoparticles on TiO_2. The increase of the OH group bands indicates the generated H_2O adsorbs on the catalyst surface (TiO_2). Reaction condition: CO_2 10 ml/min, H_2 10 ml/min (pre-treatment H_2 20 ml/min, 150 ºC, 1h.)

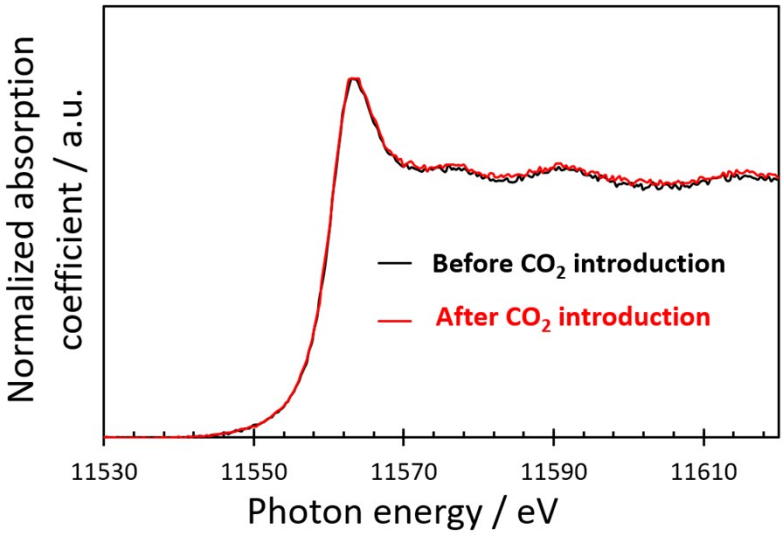

Fig. S6 *In situ* Pt L_3-edge XANES spectra of $Mo_4Pt_8O_x$ subnanoparticles supported on TiO_2 at room temperature.

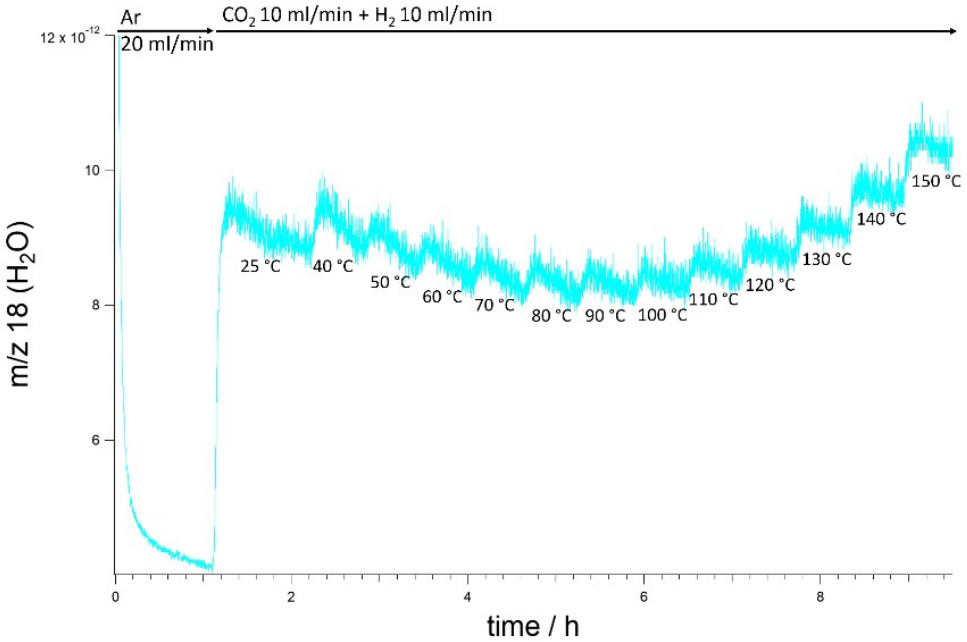

Fig. S7 The desorbed H_2O signals monitored using a quadrupole mass spectrometer. At slightly higher temperature like 40 ºC, the m/z 18 intensity increased, indicating the detection of generated H_2O from reaction.

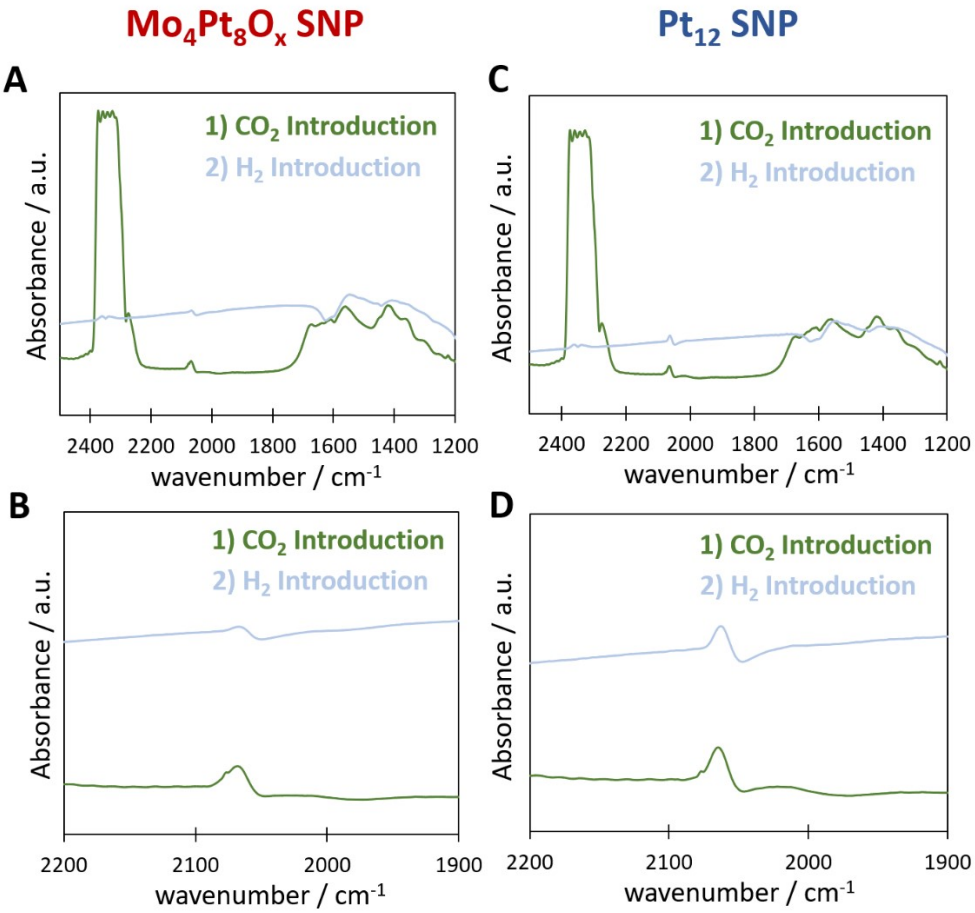

Fig. S8 *In situ* DRIFTS spectra comparison between $Mo_4Pt_8O_x$ (**A**, **B**) and Pt_{12} (**C**, **D**) subnanoparticles supported on TiO_2.

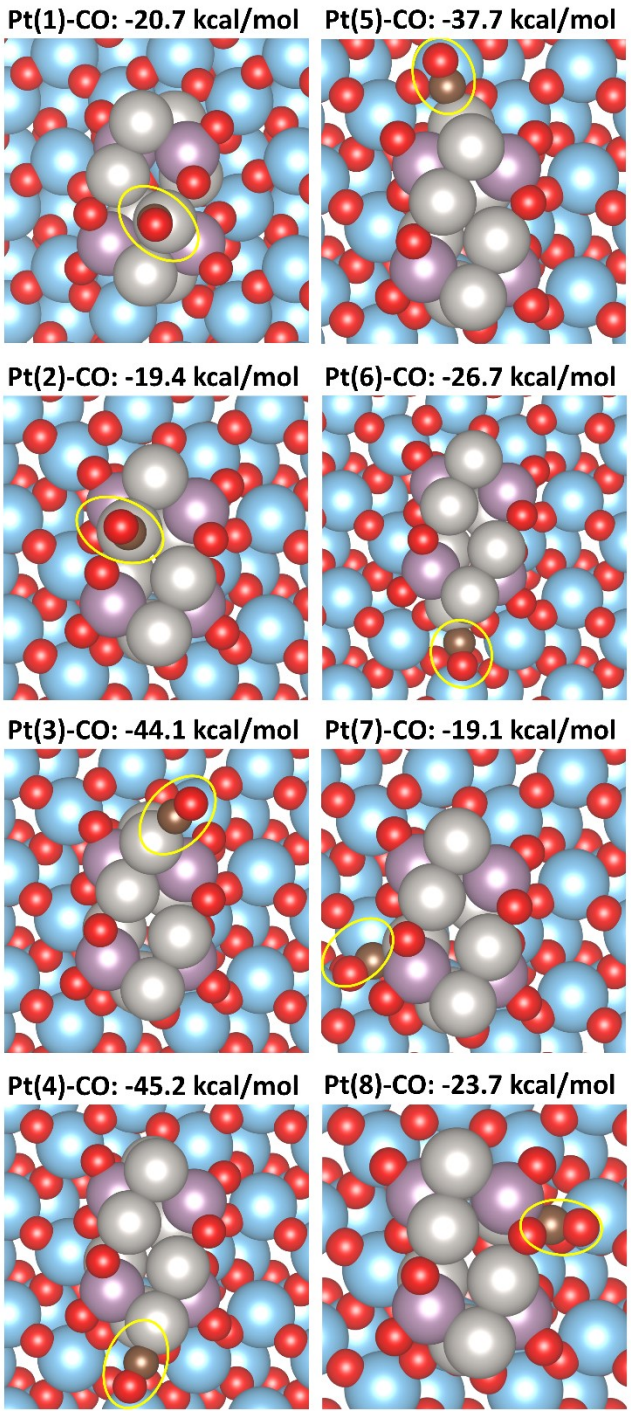

Fig. S9 DFT calculations of Pt-CO adsorption energies on $Mo_4Pt_8O_8/TiO_2(101)$ (Mo: purple, Pt: silver, C: brown, O: red, Ti: blue).

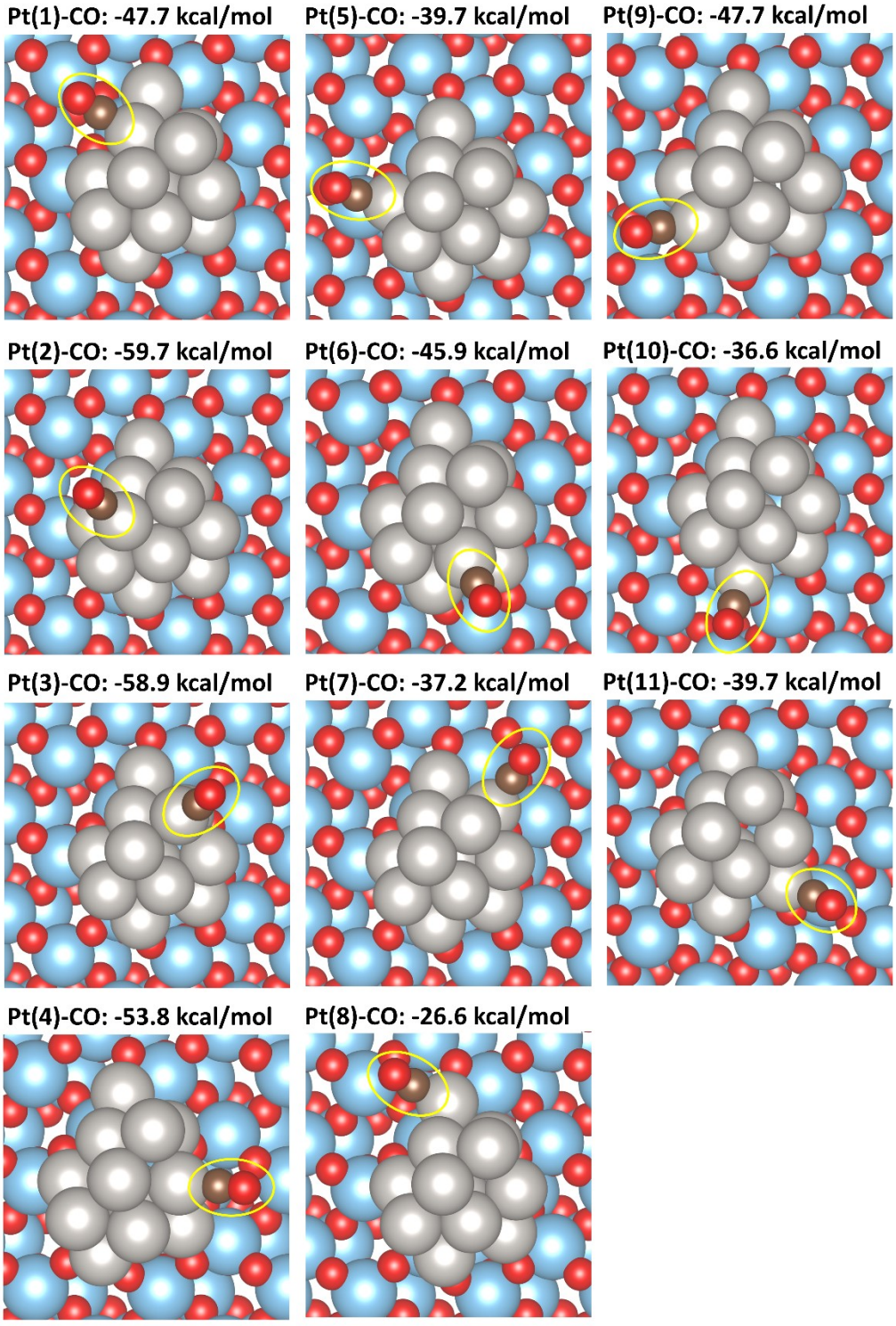

Fig. S10 DFT calculations of Pt-CO adsorption energies on $Pt_{12}/TiO_2(101)$ (Mo: purple, Pt: silver, C: brown, O: red, Ti: blue).

REFERENCES

1. Enoki, H. Katoh and K. Yamamoto, *Org. Lett.*, 2006, **8(4)**, 569-571.
2. M. Wakizaka, T. Imaoka and K. Yamamoto, *Dalton Trans.*, 2019, **48**, 14261-14268.
3. M. Wakizaka, H. Muramatsu, T. Imaoka and K. Yamamoto, *Eur. J. Inorg. Chem.*, 2020, **18**, 1759-1762.
4. T. Taguchi, T. Ozawa and H. Yashiro, *Phys. Scr.*, 2005**, T115**, 205-206.
5. A. Jain, S. P. Ong, G. Hautier, W. Chen, W. D. Richards, S. Dacek, S. Cholia, D. Gunter, D. Skinner, G. Ceder and K. A. Persson, *APL Mater.*, 2013, **1**, 011002.
6. G. Kresse and J. Furthmüller, *Phys. Rev. B* 1996, **54**, 11169-11186.
7. G. Kresse and J. Furthmüller, *Comput. Mater. Sci.*, 1996, **6(1)**, 15-50.
8. G. Kresse and J. Hafner, *Phys. Rev. B*, 1994, **49**, 14251-14269.
9. G. Kresse and J. Hafner, *Phys. Rev. B*, 1993, **47**, 558-561.
10. G. Kresse and D. Joubert, *Phys. Rev. B*, 1999, **59**, 1758-1775.
11. P. E. Blöchl, *Phys. Rev. B*, 1994, **50**, 17953-17979.
12. J. P. Perdew, K. Burke and M. Ernzerhof, *Phys. Rev. Lett.*, 1996, **77**, 3865-3868.